2025

Superconducting Linear Generators for Wave Energy Converters: A Novel Switched Reluctance Design with Optimized AC Loss Management

M. BLANCO, J. NÁJERA, G. NAVARRO, M. LAFOZ, E. RAUSELL, V. URDA, L. GARCÍA-TABARÉS, J. MUNILLA.

This is a pre-print version of a paper and it is not the final version as appearing in the Vol. 16 (2025): Proceedings of the European Wave and Tidal Energy Conference (L. M. de Carvalho Gato (Ed.), "Offline version of the Proceedings of 16th EWTEC 2025, Funchal, 7-11 September 2025", *Proc. EWTEC*, vol. 16, Oct. 2025)**.**

How to Cite this article:

Blanco, Marcos, Jorge Najera, Gustavo Navarro, Marcos Lafoz, Eduardo Rausell, Valentin Urda, Luis García-Tabares, and Javier Munilla. 2025. "Superconducting Linear Generators for Wave Energy Converters: A Novel Switched Reluctance Design with Optimized AC Loss Management." In Proceedings of the European Wave and Tidal Energy Conference. Vol. 16. https://doi.org/10.36688/ewtec-2025-925..

DOI https://doi.org/10.36688/ewtec-2025-925

LINK: https://submissions.ewtec.org/proc-ewtec/article/view/925

THIS RESEARCH, DEVELOPED UNDER THE PROYECTS:

** SETITAN (ID: 764014), HAS RECEIVED FUNDING FROM EUROPEAN UNION'S HORIZON 2020 RESEARCH AND INNOVATION PROGRAMME UNDER H2020-EU.3.3.2. - LOW-COST, LOW CARBON ENERGY SUPPLY (LCE-07-2016-2017).*

** MARES (ID: 101172746; HTTPS://DOI.ORG/10.3030/101172746), HAS RECEIVED FUNDING FROM EUROPEAN UNION'S HORIZON EUROPE RESEARCH AND INNOVATION PROGRAMME UNDER HORIZON-CL5-2024-D3-01-10 - NEXT GENERATION OF RENEWABLE ENERGY TECHNOLOGIES (HORIZON-CL5-2024-D3-01)*

Superconducting Linear Generators for Wave Energy Converters: A Novel Switched Reluctance Design with Optimized AC Loss Management

M. Blanco, J. Nájera, G. Navarro, M. Lafoz, E. Rausell, V. Urda, L. García-Tabarés, J. Munilla

Abstract— **The development of Power Take-Off (PTO) systems is crucial for the progress of wave energy technologies. Among the different PTO concepts, direct-drive systems based on linear electrical generators stand out due to their simplicity, robustness, and efficiency, as they minimize energy transformations. Despite their advantages, linear electrical generators face significant challenges, particularly in terms of force density and reactive power capability. These limitations are most evident at low operational speeds, where high currents are required to generate adequate forces, leading to significant Joule losses. Furthermore, the management of reactive power for implementing advanced control strategies, such as reactive or pseudo-optimal wave energy extraction, is hindered by constant energy dissipation. This is particularly problematic at null or low velocities, where Joule losses persist regardless of speed, limiting the use of reactive power.**

Superconducting technology has emerged as a promising solution to these challenges by significantly improving force density while reducing Joule losses. However, the cryogenic systems required for maintaining superconducting conditions impose strict constraints, as all conductor losses, including AC losses associated with oscillating currents, must be minimized. In this context, the paper describes a novel concept for a linear generator based on switched reluctance and superconducting coils, protected under a patented design. To address the issue of AC losses in superconducting cables, we introduce an innovative control strategy for the electronic converter associated with the generator. This strategy is designed to minimize current ripple in the generator phases, reducing oscillation frequencies and, consequently, AC losses.

The proposed approach employs a single-pulse switching strategy, where each phase of the converter is activated and deactivated without intermediate semiconductor switching. This eliminates additional ripple in the phase currents. To regulate the force amplitude, the voltage of the DC link connected to the converter is controlled, enabling precise force modulation.

The paper provides a comprehensive description of the switching strategy and evaluates its performance under oscillatory motion conditions typical of wave energy converters (WECs). A detailed comparison with conventional strategies demonstrates the proposed approach's potential to enhance generator efficiency, reduce losses, and improve overall performance. This work highlights the feasibility of integrating superconducting direct-drive PTO systems into WECs, paving the way for more efficient and reliable wave energy technologies.

Keywords—Power take-off, superconducting linear electric machine, power electronics.

I. INTRODUCTION

Wave energy is a promising renewable energy source due to its abundant availability, predictability, and low environmental impact [1–3]. However, efficiently converting wave energy into electricity remains a significant technological challenge due to the irregular and oscillatory nature of ocean waves, as well as economic factors [ref]. The Power Take-Off (PTO) system is a key element in this process, as it transforms the mechanical energy extracted from the waves into usable electrical power. The development of efficient and reliable PTO systems is essential for the advancement of wave energy technologies [4].

Despite their potential, conventional PTOs face several

This research, developed under the Projects SETITAN (ID: 764014), has received funding from European Union's Horizon 2020 research and innovation programme under H2020-EU.3.3.2. - Low-cost, low carbon energy supply (LCE-07-2016-2017) and MARES (ID: 101172746), has received funding from European Union's Horizon Europe research and innovation programme under HORIZON-CL5-2024-D3-01-10 - Next generation of renewable energy technologies.

All the authors (M.B., J.N., G.N., M.L., E.R., V.U., L.G., and J.M.) are with the Centro de Investigaciones Energéticas, Medioambientales, y Tecnológicas (CIEMAT), Avda. Complutense, no. 40, 28045, Madrid (Spain) (e-mail M.B.: marcos.blanco@ciemat.es).

Digital Object Identifier: https://doi.org/10.36688/ewtec-2025-925

challenges, including force density limitations, energy losses due to the Joule effect, and the complexity of reactive power management [5–7]. These issues are particularly critical in direct-drive PTOs, where the generator must operate efficiently at low speeds while maintaining high force output.

Traditional linear generators often struggle with high losses, large system sizes, and limited operational efficiency across varying wave conditions [4,5]. Superconducting technology offers a promising solution to these challenges [8,9]. By incorporating superconducting coils, it is possible to significantly increase force density while eliminating DC conduction losses, thus enhancing overall efficiency. However, the integration of superconductors requires advanced cryogenic cooling systems and effective management of AC losses caused by oscillating currents. Addressing these limitations is crucial for the feasibility of superconducting PTOs [9,10].

This paper presents a novel an innovative control strategy for a Superconducting Cylindrical Switched Reluctance Machine (SCSRM) intended for wave energy conversion. The control is aimed at minimizing AC losses in superconducting coils while improving efficiency and reliability. By employing a single-pulse switching strategy, the system reduces current ripple and associated oscillation frequencies, mitigating energy losses compared to conventional hysteresis-band control methods [11,12].

This study has been developed under the funding of MARES Horizon Europe project, and it builds upon previous advancements in SEATITAN H2020 [13] project in superconducting direct-drive PTOs, integrating insights from both conventional PTO systems and cutting-edge research in superconducting technologies. These projects and other European Union-funded initiatives have demonstrated the feasibility of superconducting linear generators for wave energy applications [10,14]. Additionally, previous research on non-superconducting PTOs [15,16] has provided a critical benchmark for evaluating the benefits and trade-offs of incorporating superconducting materials into PTO design.

The paper is structured as follows: Section II describes the design and operation of the SCSRM and its associated power electronics system, along with the novel control strategy. Section III presents the simulation model of the system. In Section IV, the system is evaluated through simulations in MATLAB/Simulink, and the results are discussed and compared. The paper concludes with a summary of the findings.

II. PTO Description: Superconducting Linear Electric Machine

In this section, we present the selected superconducting electric generator for the PTO system, along with its associated power electronics topology and both the traditional and proposed control strategies for WECs.

A. *Superconducting electric machine proposed*

The selected PTO electric generator is the Superconducting Cylindrical Switched Reluctance Machine (SCSRM). This topology has been developed in previous works [refs] to maximize efficiency and address common challenges in WECs.

As illustrated in Fig.1, [9,17] the machine is enclosed within a flexible cryostat, which consists of upper and lower bellows attached to a central stationary body. This central body houses the stator, which contains superconducting coils and is surrounded by a radiation screen. In contrast, the translator is mounted on the moving components of the cryostat while remaining thermally insulated from them. Fundamentally, this configuration should be considered a reciprocating machine with a limited stroke, rather than a conventional linear machine with unrestricted displacement.

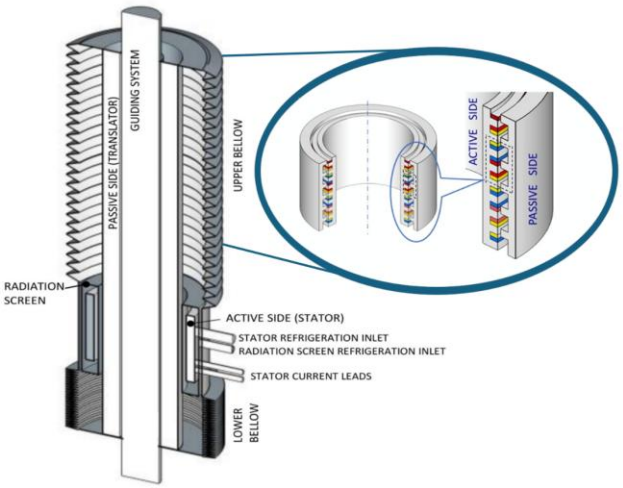

Figure 1. General view of the complete SCSRM and its cryostat

The SCSRM comprises an active external component and a passive internal component. Its modular architecture, where each "unitary machine" can be stacked to meet varying power requirements, provides scalability and aligns with common WEC designs. The cylindrical geometry ensures balanced operation by eliminating lateral forces and avoids limitations associated with the superconducting bending radius.

Using a superconducting PTO offers significant advantages. Superconducting winding exhibits zero DC electrical resistance, eliminating conduction losses and enabling near-ideal efficiency. This efficiency allows the PTO to fully harness the available force across a wide broader range of operating conditions. For example, while a conventional PTO with 75% efficiency can extract maximum power only within a narrow band of wave periods, a superconducting PTO at 100% efficiency significantly expands this range. By minimizing energy losses associated with reactive components, the superconducting system maximizes power extraction

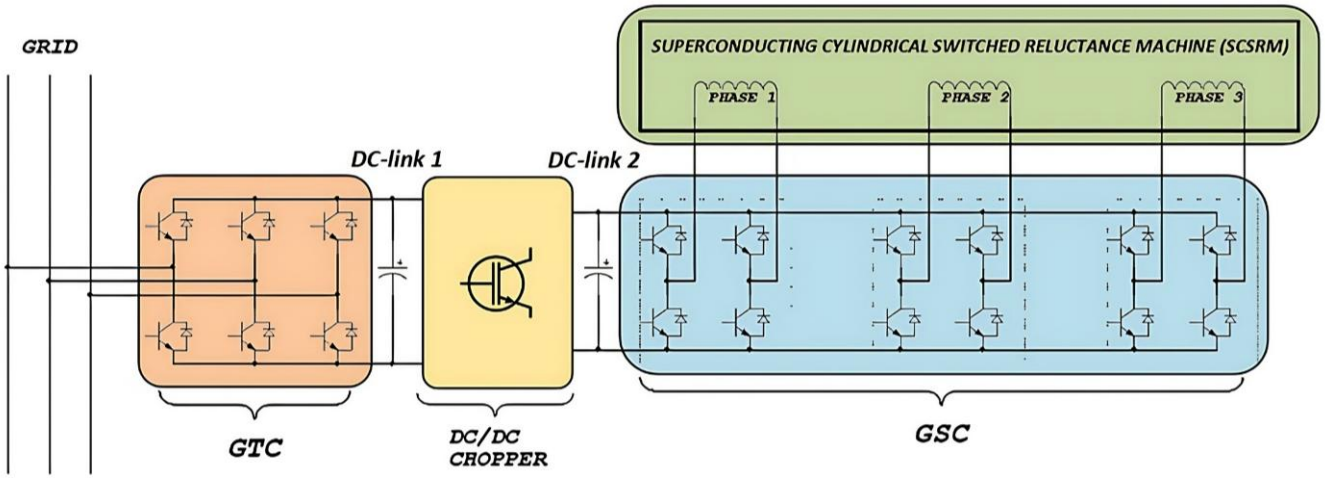

Figure 2. Complete scheme of the proposed power electronics system.

across varying wave conditions. This capability enables the system to operate closer to the theoretical maximum of the Power-Wave Period curve. As a result, it enhances energy capture across a wider spectrum of sea states, improving overall performance and reliability in wave energy conversion.

Another significant advantage of employing a superconducting machine is the considerable reduction in weight, which results from the increased number of ampere-turns. Unlike conventional conductors, superconducting wires can sustain exceptionally high current densities, often exceeding those of standard conducting wires by two orders of magnitude. This capability leads to stronger magnetic fields and greater electromagnetic forces within the machine.

Despite its advantages, two critical challenges remain:

A. Cryogenic Cooling Requirements:

The superconducting magnet must operate at extremely low temperatures (typically 10 K or below), necessitating a sophisticated cryogenic system and advanced thermal insulation.

B. AC Losses in Superconducting Wires:

While DC losses are negligible, AC-induced losses occur due to internal electric fields and eddy currents in the metal matrix.

In this work, the authors address the issue of AC losses in superconducting machines by proposing a novel control strategy to minimize them. AC losses can be split in two components:

1. Superconductor Hysteresis Losses:

These losses are related to the magnetization process inside the superconductor and how the magnetic field penetrates the material as it increases and decreases. The equation that defines the loss density is [10,18]:

$$p_h = B_m \cdot d_f \cdot \mathrm{J_c} \cdot f/\gamma \tag{1}$$

where B_m is the amplitude of the field variation, d_f the filament diameter, $\mathrm{J_c}$ the wire critical current density, γ the wire density and f the frequency of the field alternance.

2. Inter-Filament Coupling Losses:

These losses are associated with induced currents between filaments, which are generated under a time-varying magnetic field (or transport current) excitation. The equation for the loss density is [18]:

$$p_c = (1/(2 \cdot \rho_{eff} \cdot \gamma)) \cdot (\mathrm{f} \cdot L_p \cdot B_m/\pi)^2 \tag{2}$$

where the new variables are the effective resistivity of the matrix ρ_{eff}, and the twist pith L_p.

From (1) and (2), we can simplify the equations in terms of frequency and current in (3) and (4) as follows:

$$p_h = k_h \cdot i \cdot f \tag{3}$$

$$p_c = k_c \cdot i^2 \cdot f^2 \tag{4}$$

where i is the current in the coils, k_h is the constant related to superconductor hysteresis losses, and k_c is the inter-filament coupling constant.

As seen in (3) and (4), the AC losses are highly frequency-dependent, even proportional to the square of the frequency in (4). To mitigate these losses, an innovative control strategy has been introduced for the power electronics associated with the generator. This strategy is designed to minimize current ripple in the generator phases, thereby reducing oscillation frequencies and, consequently, AC losses.

B. Power electronics and switching strategy proposed control

The power electronics system is structured into three parts, as shown in Fig.2, from the grid side to the machine side: a Grid-Tied Converter (GTC), a DC/DC chopper converter, and the Generator-Side Converter (GSC), which interfaces with the SCSRM. The GTC and the DC/DC converter are connected via DC-link 1, while the DC/DC converter and the GSC are connected via DC-link 2.

1) Grid Tied Converter (GTC)

The GTC consists of an IGBT three-phase voltage source converter (VSC) operating as an inverter. The GTC

maintains the DC-link 1 voltage at its nominal value despite power fluctuations. To transfer all active power from the SCSRM to the grid, the DC-link 1 voltage must remain constant, regulated through current control. In the dq reference frame, active power regulation is achieved by controlling the d-component of the grid current (i_{gd}), which directly influences power transfer [19].

Fig.3 depicts the GSC control scheme. The measured DC-link 1 voltage (u_{DC1}) is compared with its reference value (u_{DC1}^{ref}), and the error is processed through a PI controller to generate i_{gd}^{ref}. When power generation increases, the DC-link 1 voltage rises, triggering the control loop to adjust i_{gd}^{ref} and supply more power to the grid. The q-component of the grid current is related to the grid reactive power, in this case is set to zero ($i_{gq}^{ref} = 0$). A vector current control loop [20] ensures grid currents follow their references by comparing measured and reference values via PI controllers. This process generates the grid voltage references ($u_{g\,abc}^{ref}$), which, through a PWM, control the IGBT switching in the GTC.

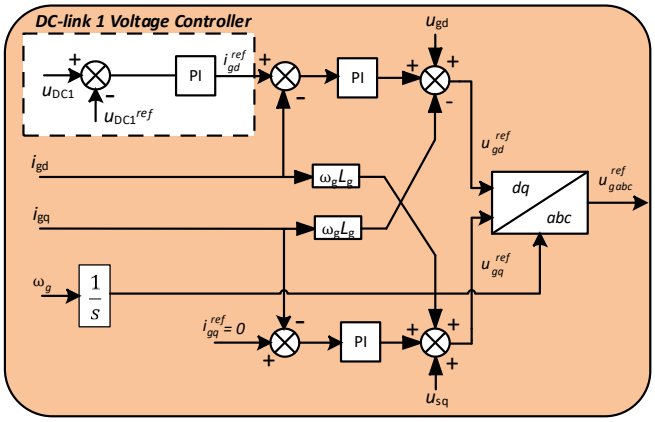

Figure 3. GTC control scheme

2) *DC/DC chopper converter*

Depending on the required DC voltage, a single GTC can be used for voltage regulation instead of combining a GTC with a DC/DC chopper. However, this approach is only viable if the voltage range required by the GSC falls within the rectified voltage limits of the GTC. Otherwise, a DC/DC chopper must be considered to ensure proper control of the superconducting machine.

Fig.4 illustrates the DC/DC chopper converter control. The measured current of the active phase of the SCSRM (i_{SCSRM}^{act}) is compared with its reference current (i_{SCSRM}^{ref}). The error is processed through a PI controller to generate the voltage reference of the DC-link 2 (u_{DC2}^{ref}). This reference is limited between its maximum (u_{DC2}^{max}) and minimum values (u_{DC2}^{min}), which correspond to the maximum supported voltage of DC-link 2 and the minimum rectified voltage of the GSC, respectively. Finally, u_{DC2}^{ref} is compared with the measured DC-link 2 voltage (u_{DC2}), and the resulting error is processed via a PI controller to obtain the duty cycle (d_{DC2}) of the converter.

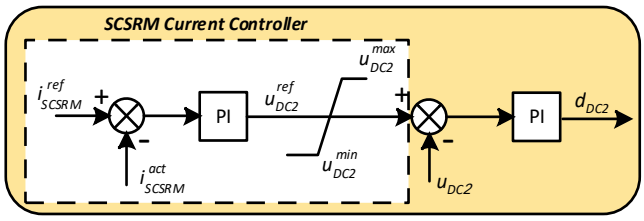

Figure 4. DC/DC chopper converter control scheme

3) *Grid Tied Converter (GTC)*

The GSC consists of three IGBT single-phase H-bridge converters sharing a common DC-link 2. Each H-bridge is assigned to a separate phase of the generator, allowing independent control of each phase.

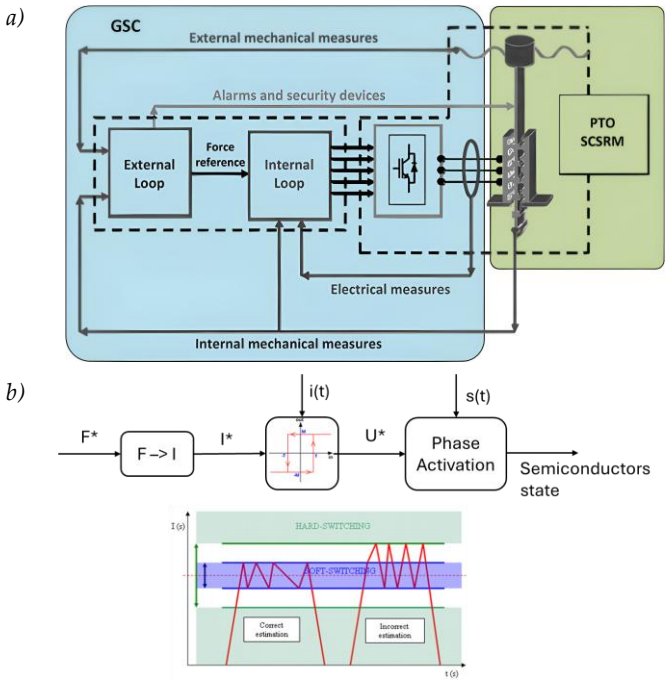

Figure 5. (a) GSC general control scheme; (b) detail of internal loop: current control (hysteresis band)

Fig.5 shows the traditional control strategy scheme of the GSC used in previous works [12,21,22], consisting of an external and an internal control loop. In the traditional strategy, the DC/DC chopper converter is not implemented, while the GTC is directly connected to the GSC via a DC link and operates as previously explained, maintaining the DC voltage controlled at a fixed reference value.

The external loop determines the force that meets the objectives in each operating state. This control loop searches for the maximum power level obtainable from the waves, with a restriction on the SCSRM force.

The internal loop imposes the SCSRM force reference obtained from the external loop, using electrical variable measurements to determine the switching states of the converter's IGBTs. This control loop first calculates the the reference force. The dependence of current on force is influenced by the characteristics of the SCSRM, as well as by the values of current and velocity. Finally, the current

reference is imposed by a hysteresis-band soft- or hard-switching strategy [21].

In this work, the proposed control strategy, as previously explained for the DC/DC chopper converter, dynamically regulates the DC-link 2 voltage to control the current in the SCSRM phase coils. Meanwhile, the GSC does not regulate the current but simply operates by activating and deactivating each phase at the correct moment, implementing a monopulse current control.

Fig. 6 illustrates the currents in the SCSRM phase coils for both hysteresis band current control and monopulse current control. At first glance, it can be seen that in monopulse current control, the current signals are smoother and have less harmonic distortion than in hysteresis band current control, highlighting the reduction in oscillation frequencies and, therefore, the reduction in AC losses.

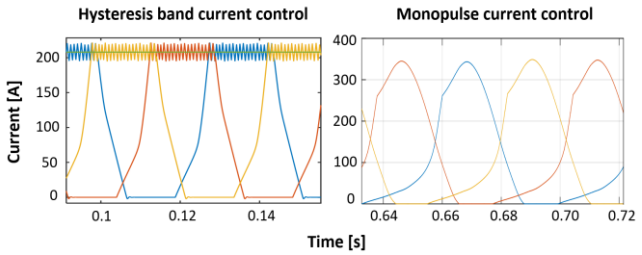

Figure 6. Currents in the SCSRM phase coils for both hysteresis band current control and monopulse current control

III. SIMULATION MODEL

To validate the proposed control strategy, a simulation model was developed in Matlab/Simulink based on the system described in Section 2.

The general block diagram of the simulation model is shown in Fig.6. The model consists of five main blocks, arranged from left to right: GTC and DC/DC chopper model, GSC model, SCSRM model, Control, and Measurements.

A. GTC and DC/DC chopper converter model

The GTC and DC/DC chopper converter are modelled as a controllable voltage source to simplify the system and speed up simulations. Given this approach, the primary components analysed in this study are the GSC and SCSRM.

As seen in block A of Fig.7, the inputs of the subsystem are the reference currents, measured currents, and velocity. Then, as depicted in Fig.4, due to the simplification of the model, u_{DC2}^{ref} is the input of the controllable voltage source, and the second loop of the control is not necessary. The output of the GTC and DC/DC chopper converter model are the electrical connections to the GSC converter.

B. GSC model

The GSC is fully modelled and consists of three single-phase IGBT H-bridges. As shown in Fig. 7, the inputs of the model (block B) are the electrical connections from the GTC and the DC/DC chopper converter model, as well as the IGBT switching patterns from the control. The outputs of the model are the electrical connections to each phase of the SCSRM.

C. SCSRM model

The electrical model of the SCSRM is based on a single-phase non-superconducting SRM. The voltage equation for each phase of the SRM can be expressed as follows [12,23]:

$$v_{ph} = R_s \cdot i_{ph} + \frac{d\lambda_{ph}(i_{ph}, \theta_{ph})}{dt} \tag{5}$$

where R_s is the stator resistance, i_{ph} is the phase current and λ_{ph} is the flux linkage per phase, which is a function of i_{ph} and the angle per phase θ_{ph}. Equation (5) is expressed in terms of λ_{ph}, however, it can also be defined in terms of transient inductance as follows:

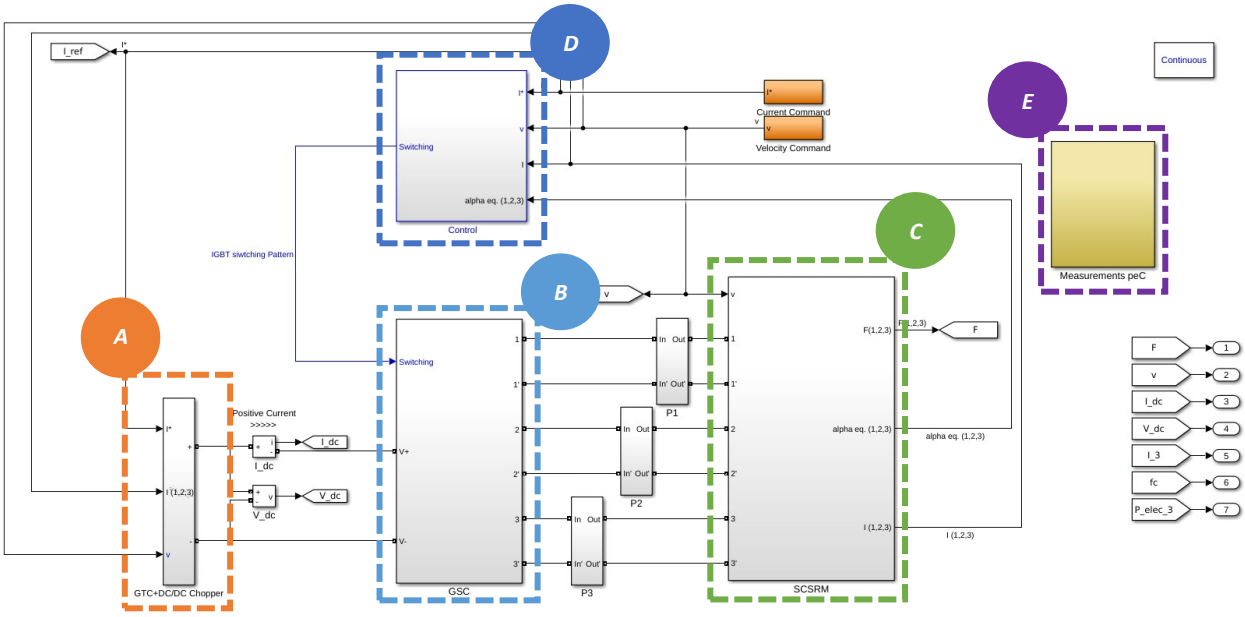

Figure 7. General block diagram of the simulati

$$v_{ph} = R_s \cdot i_{ph} + \frac{d\lambda_{ph}(i_{ph},\theta_{ph})}{di_{ph}}\frac{di_{ph}}{dt} + \frac{d\lambda_{ph}(i_{ph},\theta_{ph})}{d\theta_{ph}}\frac{d\theta_{ph}}{dt} = L_t(i_{ph},\theta_{ph})\frac{di_{ph}}{dt} + E_{ph} \quad (6)$$

where L_t is the transient inductance, which is a function of i_{ph} and θ_{ph}, and E_{ph} is the counter-electromotive force per phase.

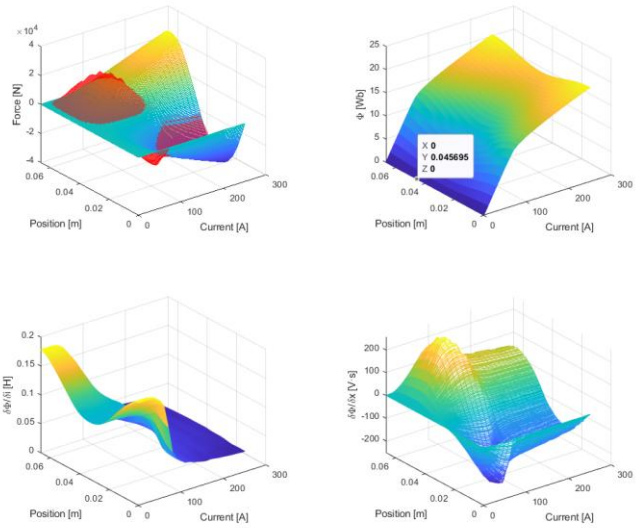

Figure 8. SRM parameters table-based approach derived from FEM

As illustrated in Fig. 8, the counter-electromotive force and inductance of the SRM are modelled using a table-based approach derived from the finite element method (FEM). The resistance in the model is considered to be nearly zero.

The inputs of the model (block C) are the electrical connections from the GSC and the velocity. The outputs of the model include the currents, forces, and the electrical equivalent angle of the machine for each phase.

D. *Control model*

In Fig. 7, Block D of the model represents the control of the GSC. As explained previously in Section II, in the proposed control scheme, the GSC does not regulate the current but simply operates by activating and deactivating each phase at the correct moment, implementing a monopulse current control. Meanwhile, the DC/DC converter regulates the DC-link 2 voltage to control the current in the SCSRM phase coils. In contrast, in the traditional control scheme, the DC/DC converter is eliminated, the GTC regulates the DC-link voltage to maintain the reference value, and the GSC controls the currents in each phase of the SCSRM.

It is important to note that the on and off angles of the GSC control have been optimized using a differential evolution algorithm [21,24,25], resulting in angle tables for each velocity, current and power value. Fig. 9 presents a colour map for a rated power operating point as a function of the switching angles Additionally, these angles have been determined while simultaneously optimizing the proportional (Kp) and integral (Ki) gains of the DC-link voltage control PI using a brute-force approach. The primary objective of this optimization process is to maximize electrical power.

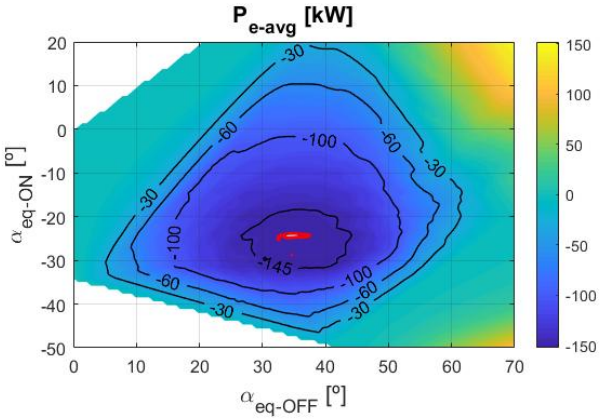

Figure 9. Rated power as a function of the switching angles

E. *Measurements*

Finally, Block E in Fig.7 represents the measurement of simulation model. This section of the model enables the evaluation and storage of all variables intended for post-processing and assessing of the results. In the context of this study, for instance, AC losses in superconducting coils are computed in a post-processing stage. The following section presents the results of the conducted simulations.

IV. RESULTS

By means of different simulations, the proposed control is compared with traditional hysteresis-band soft- and hard-switching strategy controls. The simulations are conducted for different reference currents and velocities to evaluate the results across a wide range of operating conditions.

In Fig. 10.a, the DC-link 2 voltage with the proposed control is depicted for a sinusoidal profile for velocity and force command with a period on 10 seconds and an amplitude corresponding with the rated values of the generator in velocity and force. As can be seen, the voltage varies dynamically to regulate the current in the superconducting coils, in contrast to traditional control, where the DC-link voltage remains stable. From this figure, it can be concluded that the DC/DC chopper converter is necessary due to the high voltage variations, ranging from a maximum of almost 1000 V to a minimum of approximately 550 V, which is below the rectified voltage in a 400 V grid. In addition, in Fig 10.b. the force exerted by the generator with the proposed control is depicted for sinusoidal profiles.

The results presented in Fig. 11 illustrate and compares the response of the different switching strategies for two different operating conditions. As can be seen the monopulse control strategy effectively eliminates the

current ripple observed in traditional soft- and hard-switching strategies. The characteristic triangular monopulse shape of the current waveform leads to an increased peak current compared to the average value. This current waveform is consequence of the low resistance and the natural response of a first-order LR circuit to a voltage pulse.

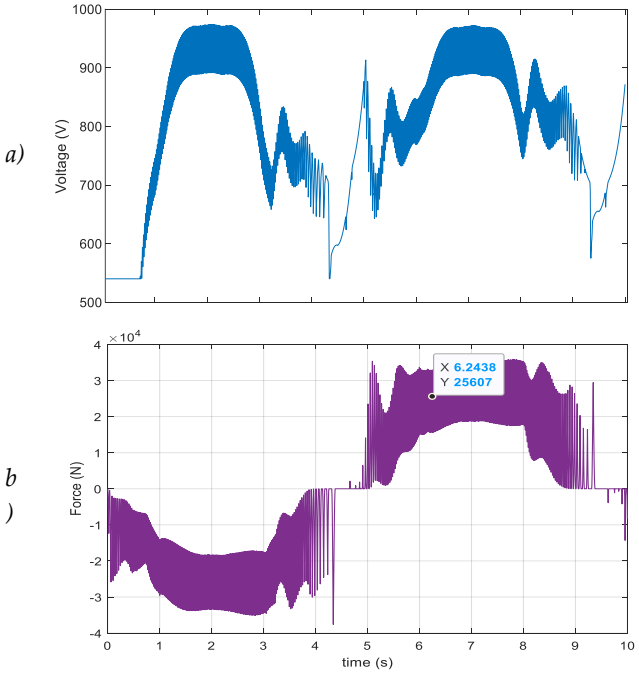

Figure 10. (a) DC-link 2 voltage dynamic variation; (b) Force

From the frequency-domain analysis, the monopulse strategy significantly reduces high-frequency components of the current, particularly around 1 kHz, which are typically present in traditional switching strategies. However, low-frequency components (approximately 15-20 Hz) remain in all cases, as they are inherently related to the phase activation and deactivation process in the SRM. These low-frequency components are tied to the machine operating principle and cannot be eliminated.

The spectral analysis of switching losses indicates that the monopulse strategy minimizes the switching frequency, thereby reducing switching losses. This potential advantage allows for the use of smaller semiconductor devices. However, due to the triangular shape of the monopulse current, the ratio of peak current to average current is close to 2, which must be considered when selecting power semiconductors. The results suggest that the monopulse strategy offers a trade-off between reduced high-frequency ripple, lower switching losses, and increased peak current, making it a promising alternative for improving the efficiency of SCSRM in WECs.

V. CONCLUSIONS

This study presents a novel SCSRM for WECs, along with an innovative control strategy aimed at minimizing AC losses in superconducting coils. The proposed monopulse current control strategy effectively reduces current ripple and high-frequency components compared to traditional control strategies, leading to lower AC losses and improved overall efficiency.

The results demonstrate that the monopulse control strategy enhances efficiency by significantly reducing high-frequency current oscillations, which in turn minimizes AC losses and improves energy conversion. Additionally, the strategy lowers switching frequencies, reducing semiconductor switching losses and allowing the use of smaller power devices. However, the triangular shape of the monopulse current waveform results in an increased peak current relative to the average value, which must be taken into account when selecting power semiconductors.

The dynamic voltage regulation provided by the DC/DC chopper converter enables precise control of superconducting coil currents, contributing to improved system performance. Simulation results validate the effectiveness of the proposed approach under various operating conditions, showcasing its potential for enhancing WEC performance.

Overall, this work highlights the feasibility of integrating superconducting direct-drive PTO systems

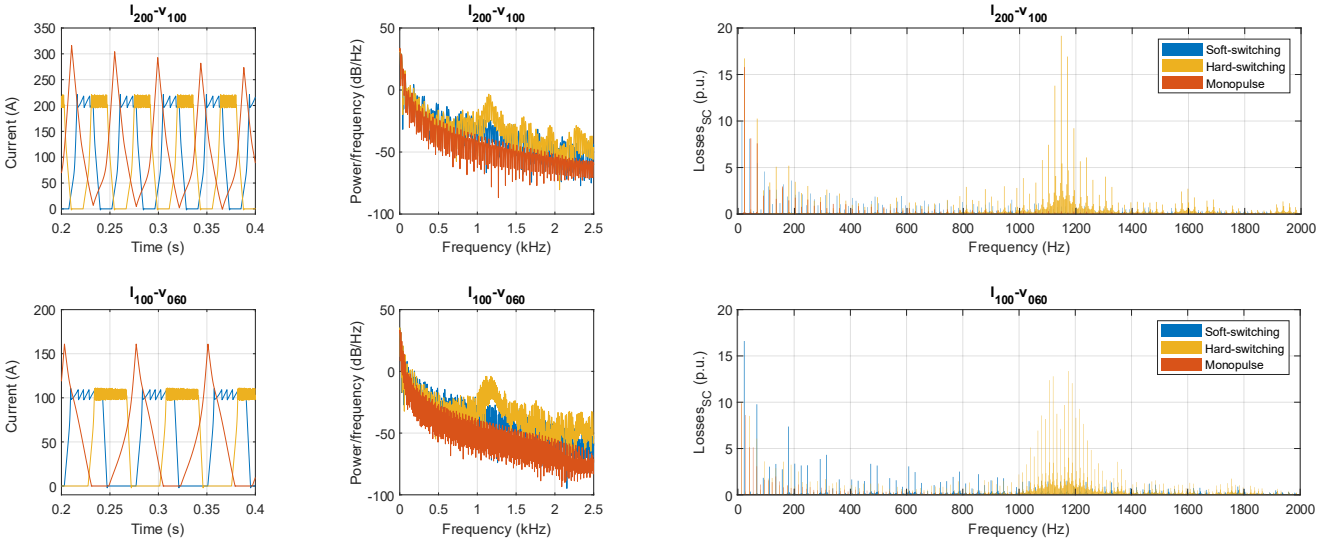

Figure 11. Comparation of the different switching strategies for two different operating conditions

into wave energy applications, contributing to the development of more efficient, reliable, and commercially viable wave energy technologies. Future research will focus on improving the model, validating it experimentally, and further optimizing the proposed control strategy.

REFERENCES

1. Falnes, J.; Kurniawan, A. Fundamental Formulae for Wave-Energy Conversion. *R. Soc. Open Sci.* **2015**, *2*.
2. Falcão, A.F. de O. Wave Energy Utilization: A Review of the Technologies. *Renew. Sustain. Energy Rev.* **2010**, *14*, 899–918, doi:10.1016/j.rser.2009.11.003.
3. *Handbook of Ocean Wave Energy*; Pecher, A., Kofoed, J.P., Eds.; Ocean Engineering & Oceanography; Springer International Publishing: Cham, 2017; Vol. 7; ISBN 978-3-319-39888-4.
4. Ruiz-Minguela, P.; Berque, J.; Villate, J.L.; Pirttimaa, L.; Gruet, R.; Noble, D.; Jeffrey, H. *Strategic Research and Innovation Agenda for Ocean Energy*; 2024;
5. Ahamed, R.; McKee, K.; Howard, I. A Review of the Linear Generator Type of Wave Energy Converters' Power Take-Off Systems. *Sustainability* **2022**, *14*, 9936, doi:10.3390/su14169936.
6. Tan, J.; Wang, X.; Polinder, H.; Laguna, A.J.; Miedema, S.A. Downsizing the Linear PM Generator in Wave Energy Conversion for Improved Economic Feasibility. *J. Mar. Sci. Eng.* **2022**, *10*, 1316, doi:10.3390/jmse10091316.
7. Brekken, T.K.A.; Yokochi, A.; von Jouanne, A.; Yen, Z.Z.; Hapke, H.M.; Halamay, D.A. Optimal Energy Storage Sizing and Control for Wind Power Applications. *IEEE Trans. Sustain. Energy* **2010**, *2*, 69–77, doi:10.1109/TSTE.2010.2066294.
8. Garcia-Tabares Rodriguez, L.; Lafoz, M.; Torres, J.J.; Obradors, D.; Blanco, M.; Najera, J.; Navarro, G.; Garcia, F.; Sanchez, A. New Type of Linear Switched Reluctance Generator for Wave Energy Applications. *IEEE Trans. Appl. Supercond.* **2020**, *30*, 1–1, doi:10.1109/TASC.2020.2981900.
9. Blanco, M.; Torres, J.; Santos-Herrán, M.; García-Tabarés, L.; Navarro, G.; Nájera, J.; Ramírez, D.; Lafoz, M. Recent Advances in Direct-Drive Power Take-Off (DDPTO) Systems for Wave Energy Converters Based on Switched Reluctance Machines (SRM). In *Ocean Wave Energy Systems. Ocean Engineering & Oceanography, vol 14*; Samad, A., Sannasiraj, S., Sundar, V., Halder, P., Eds.; Springer, Cham, 2022; pp. 487–532.
10. Tropeano, M.; Garcia-Tabarés, L.; Blanco, M.; Torres Miranda, J.; Obradors, D. Conceptual Design of a Superconducting Power Take Off within the SEATitan Project. In Proceedings of the Applied Superconductivity Conference (ASC 2020); 2020; p. Submited-reviewing.
11. Blanco, M.; Mantellini, M.; Torres, J.; Navarro, G.; Santos, M.; Najera, J.; Morici, R.; Lafoz, M. Design and Control of a Modular Power Electronic Back to Back Converter Suitable for Wave Energy Harvesting Applications. In Proceedings of the 20h European Conference on Power Electronics and Applications (EPE'20 ECCE Europe); Lyon, France, 2020; p. SUBMITTED-In REVIEW.
12. Krishnan, R. (Ramu); CRC Press. *Switched Reluctance Motor Drives : Modeling, Simulation, Analysis, Design, and Applications*; CRC Press, 2001; ISBN 1420041649.
13. SeaTitan H2020 Project - 764014 Available online: https://seatitan.eu/ (accessed on 16 April 2021).
14. Jin, J.X.; Zheng, L.H.; Guo, Y.G.; Zhu, J.G. Performance Characteristics of an HTS Linear Synchronous Motor With HTS Bulk Magnet Secondary. *IEEE Trans. Ind. Appl.* **2011**, *47*, 2469–2477, doi:10.1109/TIA.2011.2168934.
15. García, F.; Lafoz, M.; Blanco, M.; García-Tabares, L. Efficiency Calculation of a Direct-Drive Power Take-Off. In Proceedings of the Proc. of the 9th European Wave and Tidal Energy Conference (EWTEC); Southamptom, UK, 2011.
16. Lafoz, M.; Blanco, M.; Navarro, G.; Najera, J.; García-Tabares, L. Novel Proposal of PTO Direct-Drive Linear Generator, an Azimuthal Multi-Translator Switched Reluctance Machine (AMSRM): Mechanical, Characterization and Performance Tests. *Proc. Eur. Wave Tidal Energy Conf.* **2023**, *15*, doi:10.36688/ewtec-2023-308.
17. García-Tabarés, L.; Munilla, J.; López de Toledo, C.; García, F.; Sarmiento, G.; Sanz, S. ALTERNATIVE MOVEMENT SUPERCONDUCTIVE LINEAR ELECTRIC MACHINE 2020.
18. Iwasa, Y. *Case Studies in Superconducting Magnets: Design and Operational Issues: Second Edition*; Springer US, 2009; ISBN 9780387097992.
19. Rausell, E.; Navarro, G.; Lafoz, M.; Arnaltes, S.; Rodríguez, J.L.; Blanco, M.; Nájera, J. Analysis of Using MMC Topologies for the Direct Integration of Renewable Generation with Modular Electrolyzers. In Proceedings of the 2023 25th European Conference on Power Electronics and Applications (EPE'23 ECCE Europe); IEEE, September 4 2023; pp. 1–8.
20. Rausell, E.; Arnaltes, S.; Rodríguez, J.L.; Lafoz, M.; Navarro, G. Control of Wind Energy Conversion Systems with Permanent Magnet Synchronous Generator for Isolated Green Hydrogen Production. *Int. J. Hydrogen Energy* **2025**, *107*, 241–251, doi:10.1016/j.ijhydene.2024.06.347.
21. Blanco, M.; Navarro, G.; Lafoz, M. Control of Power Electronics Driving a Switched Reluctance Linear Generator in Wave Energy Applications. In Proceedings of the Proceedings of the Power Electronics and Applications, 2009. EPE '09. 13th European Conference on; IEEE, 2009; pp. 1–9.
22. Mantellini, M.; Morici, R.; Blanco, M.; Lafoz, M.; Navarro, G.; Torres, J.; Najera, J.; Santos, M. Design and Control of a Modular Power Electronic Back-to-Back Converter for Wave Energy Harvesting Applications. In Proceedings of the 2020 22nd European Conference on Power Electronics and Applications (EPE'20 ECCE Europe); IEEE, September 2020; p. P.1-P.10.
23. Ilic'-Spong, M.; Marino, R.; Peresada, S.; Taylor, D. Feedback Linearizing Control of Switched Reluctance Motors. *IEEE Trans. Automat. Contr.* **1987**, *32*, 371–379, doi:10.1109/TAC.1987.1104616.
24. Mantellini, M.; Morici, R.; Blanco, M.; Lafoz, M.; Navarro, G.; Zarri, L. Design and Testing of a Modular Back-to-Back Power Electronics Converter for Wave Energy Harvesting. In Proceedings of the 2021 IEEE Energy Conversion Congress and Exposition (ECCE); IEEE, October 10 2021; pp. 274–281.
25. Blanco, M.; Santos-Herran, M.; Navarro, G.; Torres, J.J.; Najera, J.; García-Tabarés, L. Simplified Model of a Novel Direct-Drive PTO Based on an Azimuthal Linear Switched Reluctance Generator. In Proceedings of the Proc. of the 14th European Wave and Tidal Energy Conference (EWTEC); EWTEC: Plymouth, 2021.